Eur J Nucl Med Mol Imaging (2010) 37:1903–1908
DOI 10.1007/s00259-010-1480-7

ORIGINAL ARTICLE

Real-time breath-hold triggering of myocardial perfusion imaging with a novel cadmium-zinc-telluride detector gamma camera

Ronny R. Buechel · Aju P. Pazhenkottil · Bernhard A. Herzog · Lars Husmann · René N. Nkoulou · Irene A. Burger · Ines Valenta · Christophe A. Wyss · Jelena R. Ghadri · Philipp A. Kaufmann

Received: 1 December 2009 / Accepted: 13 April 2010 / Published online: 2 June 2010

Abstract
Purpose The aim of this study was to assess the ability of real-time breath-hold-triggered myocardial perfusion imaging (MPI) using a novel cadmium-zinc-telluride (CZT) gamma camera to discriminate artefacts from true perfusion defects.
Methods A group of 40 patients underwent a 1-day ^{99m}Tc-tetrofosmin pharmacological stress/rest imaging protocol on a conventional dual detector SPECT gamma camera with and without attenuation correction (AC), immediately followed by scanning on an ultrafast CZT camera with and without real-time breath-hold triggering (instead of AC) by intermittent scanning confined to breath-hold at deep inspiration (using list mode acquisition). We studied the use of breath-hold triggering on the CZT camera and its ability to discriminate artefacts from true perfusion defects using AC SPECT MPI as the reference standard. Myocardial tracer uptake (percent of maximum) from CZT was compared to AC SPECT MPI by intraclass correlation and by calculating Bland-Altman limits of agreement.
Results AC of SPECT MPI identified 19 apparent perfusion defects as artefacts. Of these, 13 were correctly identified and 4 were partially unmasked (decrease in extent and/or severity) by breath-hold triggering of the CZT scan. All perfusion defects verified by SPECT MPI with AC were appropriately documented by CZT with and without breath-hold triggering. This was supported by the quantitative analysis, as the correlation (r) of myocardial tracer uptake between CZT and AC SPECT improved significantly from 0.81 to 0.90 ($p<0.001$) when applying breath-hold triggering. Similarly, Bland-Altman limits of agreement were narrower for CZT scans with breath-hold triggering.
Conclusion This novel CZT camera allows real-time breath-hold triggering as a potential alternative to AC to assist in the discrimination of artefacts from true perfusion defects.

Keywords Ultrafast cardiac gamma camera · Myocardial perfusion imaging · SPECT · Breath-hold triggering · Cadmium-zinc-telluride

Introduction

Myocardial perfusion imaging (MPI) plays a key role in the noninvasive assessment of cardiac disease including prediction of prognosis and choice of adequate treatment strategies in patients with known or suspected ischaemic coronary artery disease (CAD) [1]. However, although MPI is a valuable clinical tool, it is nevertheless subject to a variety of artefacts and potential pitfalls, which may affect its clinical utility [2]. Common sources of artefacts in MPI studies are attenuation of photons by the patient's body as well as prominent subdiaphragmatic gastrointestinal activity which typically interferes with the adjacent inferior myocardial wall and may either lead to increased activity (due to spill-over) or to apparently decreased activity (caused by hot spots).

Ronny R. Buechel and Aju P. Pazhenkottil contributed equally to this work.

R. R. Buechel · A. P. Pazhenkottil · B. A. Herzog · L. Husmann · R. N. Nkoulou · I. A. Burger · I. Valenta · C. A. Wyss · J. R. Ghadri · P. A. Kaufmann (✉)
Cardiac Imaging, University Hospital Zurich,
Ramistrasse 100,
CH-8091 Zurich, Switzerland
e-mail: pak@usz.ch

P. A. Kaufmann
Zurich Center for Integrative Human Physiology (ZIHP),
University of Zurich,
Zurich, Switzerland

Several strategies to address these problems and to discriminate artefacts from perfusion defects have been proposed, such as scanning in the prone position [3], integrating findings from gated SPECT [4], and attenuation correction (AC) using line sources [5] or low-dose CT [6]. As an alternative for improving SPECT image quality, respiratory gating has been suggested [7–11], but has remained challenging due to the step-and-shoot acquisition mode with SPECT gamma cameras with rotating detectors.

The introduction of a novel generation of gamma cameras using cadmium-zinc-telluride (CZT) detectors may at least in part help to overcome these drawbacks and limitations. The miniaturized CZT detectors and a multipinhole design enables alignment of the detectors around the patient, thus covering the entire heart at all times and rendering camera rotation around the patient unnecessary thus allowing a more than fivefold shortening of the scan time [12, 13]. In addition, this enables intermittent scanning which, in combination with list-mode acquisition, allows breath-hold triggering.

Thus, the aim of the present study was to assess the ability of real-time breath-hold triggering of CZT scanning to discriminate MPI artefacts from true perfusion defects using AC of SPECT MPI as the reference standard.

Materials and methods

Study protocol and image acquisition

A group of 40 patients referred for SPECT MPI for evaluation of CAD underwent a 1-day ^{99m}Tc-tetrofosmin stress/rest MPI protocol as suggested by the guidelines of the European Association of Nuclear Medicine [14]. Scanning for stress and rest was performed first on a conventional dual detector SPECT gamma camera (Ventri, GE Healthcare). The scan duration was 14 min and 52 s for both stress and rest. Each scan was repeated within minutes on an ultrafast CZT camera (Discovery 530 NMc, GE Healthcare) once with regular acquisition, i.e. with normal breathing, and a second time with real-time breath-hold triggering. Therefore, patients were repeatedly told to perform a breath-hold at a deep inspiration level while scanning was manually initiated after end inspiration to ensure confinement of the acquisition to breath-hold at deep inspiration. After scanning at breath-hold for a time (10–20 s) that had been individually determined according to the patient's ability, acquisition was manually interrupted and the patient was allowed to breathe normally before continuing the scan. This sequence was repeated until an overall scan duration of 3 min for stress and 2 min for rest was reached, as previously established for this camera [12, 13].

Pharmacological stress was induced by standard adenosine or dobutamine infusion [14]. ^{99m}Tc-tetrofosmin was injected after 3 min of induced stress. The injection was followed by a wait of 90 min before image acquisition on both cameras. Rest MPI was performed thereafter with the identical acquisition protocol after injection of a three times higher dose of ^{99m}Tc-tetrofosmin.

Acquisition on the conventional dual head SPECT camera was performed using a low-energy high-resolution collimator, a 20% symmetric window at 140 keV, a 64×64 matrix, and an elliptical orbit with step-and-shoot acquisition at intervals of 3° over an arc of 180° (45° anterior oblique to 45° left posterior oblique) with 30 steps (60 views). Electrocardiogram-gated scans were acquired using 16 bins. The scan time was set to 25 s per frame for stress and rest, resulting in a total scan time (including interstep rotation time) of 14 min and 52 s according to the guidelines [14].

Scans on the CZT camera were acquired using a multipinhole collimator (effective diameter aperture 5.1 mm) and 19 stationary detectors simultaneously imaging 19 views of the heart. Each detector contained 32×32 pixelated (2.46×2.46 mm) CZT elements. Image acquisition was performed using list mode. A 10% symmetrical energy window at 140 keV was used. Electrocardiogram-gated scans were acquired using 16 bins. Scans on the CZT camera were acquired over 3 min for stress and 2 min for rest, as recently established [12, 13]. As the CZT detectors are aligned around the patient, covering the entire heart, acquisition of all cardiac views simultaneously is possible, as opposed to the SPECT acquisition.

The study protocol was approved by the local ethics committee and written informed consent was obtained from every patient.

CT attenuation correction

To create CT AC maps all patients underwent an unenhanced 64-slice CT examination on a LightSpeed VCT Scanner (GE Healthcare) during breath-hold as previously reported [6]. The scans covered the entire heart using prospectively electrocardiogram-triggered sequential images at 75% of the R-R interval, 2.5 mm section thickness, and 0.35 s gantry rotation time at 120 kV and 200 mA, depending on the patient's body mass index (BMI). CT images were reconstructed with 5 mm thickness using a reconstruction algorithm with a 512×512 matrix and a field of view of 50×50 cm adapted to the full chest size. The reconstructed CT images were then transferred to a Xeleris workstation (GE Healthcare) for AC map creation.

MPI reconstruction

Images from the conventional SPECT camera were reconstructed with and without CT AC on a dedicated workstation using a standard iterative reconstruction algorithm with

ordered subset expectation maximization (OSEM). CZT images were reconstructed on the same workstation using a dedicated iterative algorithm with maximum likelihood expectation maximization (MLEM). Perfusion images in standard axis (short axis, vertical long axis, horizontal long axis) and polar maps of the left ventricle were obtained.

Visual analysis

Scans from both conventional SPECT and CZT were analyzed in consensus by two experienced readers blinded to any information on patient identification or the camera utilized or acquisition type. Cardiac perfusion was assessed on a per patient basis and for each vessel territory with regard to severity using a five-point scale (*1* normal, *2* equivocal, *3* perfusion defect with moderate decrease in uptake, *4* severe decrease in uptake, *5* absent) and extent using a three-point scale (*1* small, *2* moderate, *3* large), as previously reported [15]. Agreement and discrepancies in severity and extent between conventional SPECT with and without AC and between CZT with and without breath-hold triggering were recorded per patient and per coronary territory. The former served as the reference standard, as CT AC is not yet validated for this novel CZT camera system. Image quality was assessed subjectively on a four-point scale (*1* poor, *2* fair, *3* good, *4* excellent) with the following parameters being considered: myocardial count density and uniformity, endocardial and epicardial edge definition, and background noise

Quantitative analysis

The software package Myovation for Alcyone (GE Healthcare) was used for quantitative analysis off MPI polar maps using a 20-segment model for the left ventricle. Uptake was normalized to 100% peak activity and relative myocardial uptake (percent of maximum myocardial uptake) was assessed from the SPECT and CZT data for each vessel territory: left anterior descending artery (LAD), segments 1, 2, 7, 8, 13, 14, 15, 19 and 20; left circumflex artery (LCX), segments 5, 6, 11, 12, 17 and 18; right coronary artery (RCA), segments 3, 4, 9, 10 and 16. Automated analysis of gated acquisitions from high-dose (rest) scans was performed to determine left ventricular ejection fraction (LVEF).

Statistics

SPSS 17.0 (SPSS, Chicago, IL) was used for statistical testing. Quantitative variables are expressed as means±SD and categorical variables as frequencies or percentages. The correlation of tracer uptake and LVEF between AC SPECT and CZT with and without breath-hold triggering was evaluated using intraclass correlation analysis (absolute agreement) and Fisher's Z-transformation was used to compare correlation coefficients. In addition, Bland-Altman (BA) limits of agreement were calculated. *P* values less than 0.05 were considered statistically significant and the 95% confidence intervals are presented.

Results

Patient characteristics are given in Table 1. Patients were referred for nuclear MPI for the following reasons: suspected CAD (n=25, 62%), follow-up of a known CAD (n=14, 35%), preoperative risk assessment before major noncardiac surgery (n=1, 3%). In 39 patients (97%) pharmacological stress was induced with adenosine and in 1 patient (3%) with dobutamine. For stress and rest, mean doses of 327±25 MBq (range 292–414 MBq) and 940 ±47 MBq (range 900–1180 MBq) ^{99m}Tc-tetrofosmin were administered, respectively. All 40 patients underwent MPI on both cameras and real-time breath-hold triggering was successfully performed in all patients.

Visual analysis

The quality of conventional SPECT MPI scans without AC was good or excellent in 36 patients (90%) and fair in 4 patients (10%). After AC, the quality of SPECT MPI scans was good or excellent in 37 patients (93%) and fair in 3 patients (7%). The quality of CZT scans without breath-hold triggering was good or excellent in 35 patients (87%), fair in 4 patients (10%), and poor in 1 patient (3%). The quality of CZT scans with breath-hold triggering was good or excellent in 39 patients (97%) and fair in 1 patient (3%). Gastrointestinal tracer activity adjacent to the myocardial wall was seen in both SPECT and CZT scans in nine patients.

Uncorrected SPECT scans showed 19 apparent perfusion defects that were identified as artefacts after applying AC, predominantly located in the RCA territory (Fig. 1a). All 19 artefacts were also seen in the nontriggered CZT scans. With breath-hold triggering 13 apparent perfusion defects were identified as artefacts and 4 were at least partially unmasked as they were substantially decreased in extent and/or severity. One additional apparent perfusion defect, present on CZT scans but not on SPECT MPI scans, was appropriately identified as an artefact by breath-hold triggering. The latter was most successful in the RCA territory (Fig. 1b).

True myocardial perfusion defects were revealed in 16 AC SPECT MPI scans (5 fixed and 6 reversible defects) in 11 patients. All corresponding defects were equally identified by CZT scans with and without breath-hold triggering,

Table 1 Patient baseline characteristics (n=40)

Male	24 (60%)
Age (years)	
Mean±SD	66±10
Range	43–81
BMI (kg/m^2)	
Mean±SD	26±4
Range	19–34
Cardiovascular risk factors	
Obesity (BMI >30 kg/m^2)	7 (18%)
Smoking	9 (23%)
Diabetes mellitus	7 (18%)
Hypertension	27 (68%)
Dyslipidaemia	20 (50%)
Positive family history	5 (13%)
Clinical symptoms	
Typical angina pectoris	2 (5%)
Atypical chest pain	21 (53%)
Dyspnoea	3 (8%)
No cardiac symptoms	14 (35%)
Current cardiac medication	
Aspirin	21 (53%)
Beta-blocker	16 (40%)
ACE/angiotensin-II Inhibitor	17 (43%)
Statin	21 (53%)

indicating that the gain in specificity (i.e. the unmasking of apparent defects as artefacts) was not achieved at the cost of a decrease in sensitivity. Of note, five apparent defects in the RCA territory confirmed as true defects by CT AC SPECT were also identified by CZT with and without breath-hold triggering, indicating specifically in this territory, which is most prone to artefacts, that the corrections were not over-corrections. Figure 2 illustrates the impact of AC and breath-hold triggering on artefacts in SPECT MPI and CZT MPI, respectively.

Quantitative analysis

The intraclass correlation coefficient (r) comparing myocardial tracer uptake between conventional AC SPECT MPI and CZT without breath-hold triggering was 0.81 (95% CI 0.63–0.88, p<0.001) and between conventional AC SPECT MPI and CZT with breath-hold triggering was significantly better (p<0.001) at 0.90 (95% CI 0.85–0.93, p<0.001). Consequently, when comparing CZT to conventional AC SPECT scans, the BA limits of agreement for percent myocardial tracer uptake narrowed from −17% to 9% for CZT without breath-hold triggering to −12% to 8% for CZT with breath-hold triggering.

The intraclass correlation coefficient comparing LVEF between SPECT and CZT without breath-hold triggering was 0.92 (95% CI 0.84–0.96, p<0.001) and the BA limits of agreement were −17% to 12%. The correlation coefficient for the comparison between SPECT and CZT with breath-hold triggering was the same at 0.93 (95% CI 0.80–0.97, p<0.001) and the BA limits of agreement were −16% to 8% for CZT with breath-hold triggering.

Discussion

The finding of apparent perfusion defects that are in fact artefacts due to tissue attenuation and/or gastrointestinal tracer activity is not uncommon in MPI but may be overcome by appropriate AC. In the present study AC identified 19 such apparent perfusion defects on SPECT MPI as artefacts. Similarly, breath-hold triggering identified 13 of these apparent perfusion defects on the CZT scans as artefacts, and additionally led to a partial unmasking of four of the remaining six artefacts by substantially decreasing the extent

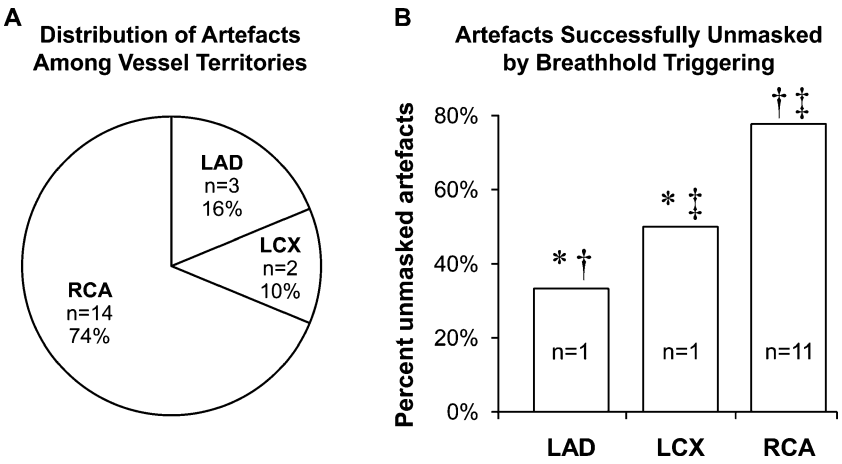

Fig. 1 Artefacts (as determined by AC SPECT MPI) were predominantly present in the RCA territory (**a**). Breath-hold triggering proved most successful in identifying artefacts in the RCA territory (**b**). (* LAD vs. LCX, non significant; † LAD vs. RCA, p<0.05; ‡ LCX vs. RCA, p<0.05)

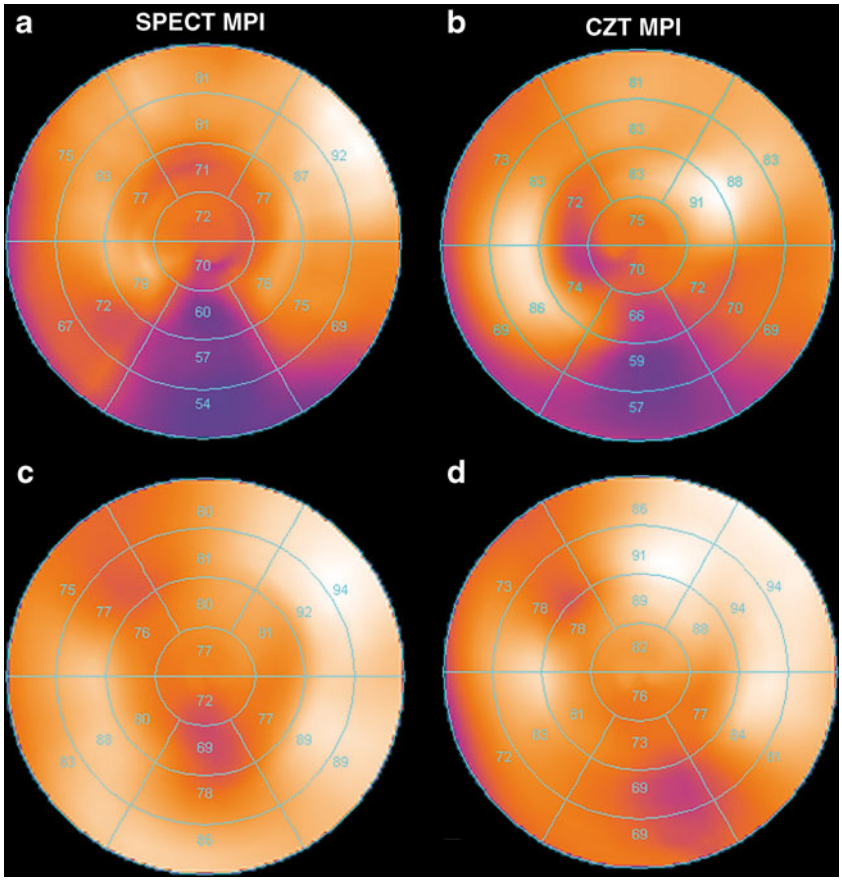

Fig. 2 SPECT MPI image without AC (**a**) and CZT MPI image without breath-hold triggering (**b**) show an apparent inferior perfusion defect which was identified as an artefact as it is not present on the SPECT MPI image after AC (**c**) or on the CZT MPI image after breath-hold triggering (**d**)

and/or severity of the apparent perfusion defect. Breath-hold triggering was most effective in patients with subdiaphragmatic tracer activity and in obese patients with attenuation artefacts in the RCA territory, where most of the artefacts where located (Fig. 1). Conversely, in the present study, CZT scans with breath-hold triggering correctly identified all perfusion defects that were confirmed as true defects by AC. Thus, applying breath-hold triggering successfully increased the specificity for discriminating true defects from artefacts without affecting sensitivity to detect defects.

Several different approaches have been described to improve reader confidence in SPECT MPI by identifying apparent defects as artefacts caused by tissue attenuation or subdiaphragmatic tracer activity. Among these, the most efficient and accurate technique is AC based on transmission data obtained either by an additional rotating isotope or by CT [14]. However, on the other hand AC can potentially introduce artefacts, particularly in the presence of subdiaphragmatic tracer activity [16]. Similarly, scanning in the prone position to correct for inferior attenuation has been associated with artefacts that are interpreted as anteroseptal defects [3].

Consequently, even when applying any of the above procedures for AC, image interpretation should still integrate all available patient information, including obesity and gender, as well as wall motion analysis from electrocardiogram-gated SPECT [4, 17], as this increases accuracy and reader confidence as to whether an apparent defect should be classified as a true defect or as an artefact. The present study demonstrated that real-time breath-hold triggering confining the image acquisition to breath-hold at deep inspiration levels may serve as an alternative to CT AC, as it unmasked the majority of artefacts. This was particularly successful in the RCA territory (79% of artefacts unmasked, Fig. 1b) where most of the attenuation artefacts were found, in line with a large body of literature (Fig. 1a) [14].

The concept of breath-hold gating is not new [7–11]. However, most previous studies have focused on retrospective respiratory gating using rotating dual head SPECT gamma cameras requiring either an increase in activity or a prolongation of the acquisition time, rendering the procedure very cumbersome. In addition, retrospective gating does not allow scanning at forced inspiration as such controlled breathing is not feasible over a prolonged period of 20 to 30 minutes. These drawbacks have so far hampered the introduction of respiratory gating for SPECT MPI into daily clinical routine. By contrast, this present study validated the use of real-time breath-hold triggering with breath hold at maximal inspiration, overcoming the above drawbacks and potentially paving the way for its introduction into clinical use.

Attenuation artefacts have for a long time been known to affect the specificity of nuclear MPI. Although recently low-dose CT has emerged as an excellent tool for accurate AC [6], the need for an integrated SPECT/CT device with higher costs or time-consuming repositioning of the patient into a stand-alone CT scanner have limited its widespread use. Similarly, the vast majority of latest generation gamma cameras with CZT detectors will not be equipped with a CT facility. Therefore, real-time CZT MPI with breath-hold triggering offers a welcome alternative to CT AC for discriminating artefacts from true perfusion defects.

It may be perceived as a limitation of this study that we did not use invasive coronary angiography as the reference standard. However, this study was aimed at evaluating the impact of real-time breath-hold triggering on MPI. We felt that it was sufficient to use a reference image modality directly reflecting myocardial perfusion, while invasive coronary angiography would have been a flawed reference standard as anatomical findings do not necessarily reflect the underlying haemodynamic situation. The use of any other non-SPECT MPI such as MRI or PET would have involved many technical differences and would have required complex protocols with coinjection of the respective flow tracer. Therefore, we used CT AC SPECT as the reference standard, as CT-based AC for SPECT has been shown to improve accuracy [18]. Finally, breath holding may potentially pose a problem in patients with dyspnoea. However, the advantage of the present protocol is that, in contrast to breath holding for CT scanning, the duration of the breath hold can be dictated by the patient's ability. This may have positively influenced patient comfort.

Conclusion

We have established a protocol for real-time breath-hold triggering of MPI on a novel CZT gamma camera as a potential alternative to AC to assist in the discrimination of artefacts caused by soft-tissue attenuation or subdiaphragmatic tracer activity from true perfusion defects.

Acknowledgments This study was supported by a grant from the Swiss National Science Foundation and by the ZIHP (Zurich Center for Integrative Human Physiology, University of Zurich, Switzerland). We would like to thank Edlira Loga and Ennio Mueller for their excellent technical support.

Disclosure The University Hospital Zurich holds a research grant with GE Healthcare.

References

1. Thomas GS, Miyamoto MI, Morello AP 3rd, Majmundar H, Thomas JJ, Sampson CH, et al. Technetium 99m sestamibi myocardial perfusion imaging predicts clinical outcome in the community outpatient setting. The Nuclear Utility in the Community (NUC) Study. J Am Coll Cardiol 2004;43:213–23.
2. Burrell S, MacDonald A. Artifacts and pitfalls in myocardial perfusion imaging. J Nucl Med Technol 2006;34:193–211.
3. Segall GM, Davis MJ. Prone versus supine thallium myocardial SPECT: a method to decrease artifactual inferior wall defects. J Nucl Med 1989;30:548–55.
4. Fleischmann S, Koepfli P, Namdar M, Wyss CA, Jenni R, Kaufmann PA. Gated (99m)Tc-tetrofosmin SPECT for discriminating infarct from artifact in fixed myocardial perfusion defects. J Nucl Med 2004;45:754–9.
5. Bailey DL, Hutton BF, Walker PJ. Improved SPECT using simultaneous emission and transmission tomography. J Nucl Med 1987;28:844–51.
6. Schepis T, Gaemperli O, Koepfli P, Ruegg C, Burger C, Leschka S, et al. Use of coronary calcium score scans from stand-alone multislice computed tomography for attenuation correction of myocardial perfusion SPECT. Eur J Nucl Med Mol Imaging 2007;34:11–9.
7. Cho K, Kumiata S, Okada S, Kumazaki T. Development of respiratory gated myocardial SPECT system. J Nucl Cardiol 1999;6:20–8..
8. Segars WP, Tsui BMW. Study of the efficacy of respiratory gating in myocardial SPECT using the new 4-D NCAT. IEEE Trans Nucl Sci 2000;47:1192–5.
9. Livieratos L, Rajappan K, Stegger L, Schafers K, Bailey DL, Camici PG. Respiratory gating of cardiac PET data in list-mode acquisition. Eur J Nucl Med Mol Imaging 2006;33:584–8.
10. Kovalski G, Israel O, Keidar Z, Frenkel A, Sachs J, Azhari H. Correction of heart motion due to respiration in clinical myocardial perfusion SPECT scans using respiratory gating. J Nucl Med 2007;48:630–6.
11. Martinez-Moller A, Zikic D, Botnar RM, Bundschuh RA, Howe W, Ziegler SI, et al. Dual cardiac-respiratory gated PET: implementation and results from a feasibility study. Eur J Nucl Med Mol Imaging 2007;34:1447–54.
12. Herzog BA, Buechel RR, Katz R, Brueckner M, Husmann L, Burger IA, et al. Nuclear myocardial perfusion imaging with a cadmium-zinc-telluride detector technique: optimized protocol for scan time reduction. J Nucl Med 2010;51:46–51.
13. Buechel RR, Herzog BA, Husmann L, Burger IA, Pazhenkottil AP, Treyer V, et al. Ultrafast nuclear myocardial perfusion imaging on a new gamma camera with semiconductor detector technique: first clinical validation. Eur J Nucl Med Mol Imaging 2010;37:773–8.
14. Hesse B, Tagil K, Cuocolo A, Anagnostopoulos C, Bardies M, Bax J, et al. EANM/ESC procedural guidelines for myocardial perfusion imaging in nuclear cardiology. Eur J Nucl Med Mol Imaging 2005;32:855–97.
15. Kovalski G, Keidar Z, Frenkel A, Israel O, Azhari H. Correction for respiration artefacts in myocardial perfusion SPECT is more effective when reconstructions supporting collimator detector response compensation are applied. J Nucl Cardiol 2009;16:949–55.
16. Pitman AG, Kalff V, Van Every B, Risa B, Barnden LR, Kelly MJ. Contributions of subdiaphragmatic activity, attenuation, and diaphragmatic motion to inferior wall artifact in attenuation-corrected Tc-99m myocardial perfusion SPECT. J Nucl Cardiol 2005;12:401–9.
17. Hesse B, Lindhardt TB, Acampa W, Anagnostopoulos C, Ballinger J, Bax JJ, et al. EANM/ESC guidelines for radionuclide imaging of cardiac function. Eur J Nucl Med Mol Imaging 2008;35:851–85.
18. Masood Y, Liu YH, Depuey G, Taillefer R, Araujo LI, Allen S, et al. Clinical validation of SPECT attenuation correction using x-ray computed tomography-derived attenuation maps: multicenter clinical trial with angiographic correlation. J Nucl Cardiol 2005;12:676–86.